NONLINEAR AERODYNAMICS OF DELTA WINGS IN COMBINED PITCH AND ROLL

ICAS-88-4.5R

J. Er-El*, D. Seter** and D. Weihs***
Faculty of Aeronautical Engineering
Technion - Israel Institute of Technology
Haifa 32000, Israel.

Abstract

This paper presents an experimental study on the effects of roll on the loading and rolling moment of a 60° swept delta wing. The experiments were carried out at angles of incidence which include cases where vortex breakdown is present on the wing ($\alpha \leq 25°$). Results indicate that when vortex breakdown is not present, the effects of roll on the wing loading and rolling moment are in reasonable agreement with predictions obtained from an approximate model. When vortex breakdown is present, the magnitude of the measured rolling moment coefficient is reduced considerably and its sign can even be altered. The changes in the rolling moment characteristics due to vortex breakdown can be attributed to the roll-induced spanwise displacement of the leading-edge vortices.

Nomenclature

- a - Parameter in the Joukowsky transformation
- c - Wing root chord
- C_{NOR} - Normal force coefficient
- $C_{NOR,1}$ - Contribution of the leading half-wing to C_{NOR}
- $C_{NOR,2}$ - Contribution of the lee half-wing to C_{NOR}
- $\bar{C}_{NOR,1}$ - $(= C_{NOR,1}/C_{NOR})$
- $\bar{C}_{NOR,2}$ - $(= C_{NOR,2}/C_{NOR})$
- C_R - Rolling moment coefficient
- C_p - Pressure coefficient, $=[(p-p_\infty)/q]$
- h - Height above the ground of the chordwise station $\bar{x}=2/3$ (see Fig. 6)
- $\bar{h}$ - Proximity ratio, $[=h/s(1)]$
- p - Pressure
- q - Dynamic pressure
- $s(\bar{x})$ - Wing local semi-span
- V_∞ - Free stream velocity
- W - Complex potential, $W=\varphi+i\psi$, (see Appendix A)
- $\bar{x}$ - Nondimensional chordwise coordinate $(\bar{x} = x/c)$
- $\bar{x}_{VB}$ - Chordwise position of VB
- $\bar{y}$ - Nondimensional local spanwise coordinate $[\bar{y} = y/s(\bar{x})]$
- α - Angle of attack
- β - Yaw angle
- Γ - Circulation of the concentrated vortex, (see Appendix A)
- ε - $(= \alpha'/tg^{-1}[s(1)/c])$, (see Appendix A)
- φ - Flow potential (see Appendix A)
- ψ - Stream function, (see Appendix A)
- ρ - Density
- ζ - $(=\xi+i\eta)$, (see Fig. 7)
- ϕ - Roll angle
- σ - $(= y + iz)$, (see Fig. 7)

Subscripts

- 1 - leading vortex
- 2 - lee vortex

Superscripts

- $'$ - conditions in the approximate model (see Appendix A)

Introduction

Combined pitch and roll (or the equivalent, combined pitch and bank) maneuvers, in addition to the classical application in takeoff and landing situations with side wind, are of cardinal importance to a super-maneuverable aircraft. When such maneuvers are executed by delta-winged aircraft, the contribution of the leading edge vortices to the wing loading, both in the symmetrical and asymmetrical cases, is significant.

Previous studies[1-2] on delta wings under combined pitch and yaw were carried out on wings having sweep angles of 75 deg[1] and 80 deg[2] and at angles of attack in which vortex breakdown (VB) is not present in the symmetrical case. These studies, which were based on flow visualization and on surface pressure measurements, indicate that yaw affects both the vortex positions and the suction they induce on the upper surface. Due to yaw, the leading vortex is displaced windward and downward while the lee vortex is displaced windward and upward. The changes in vortex positions are accompanied by an increase in the suction peak induced by the leading vortex and by a decrease in the peak induced by the lee vortex. Both studies showed that yaw stimulates

---

* Senior Lecturer
** Graduate Student
*** Professor

appearance of VB in the leading vortex. The wings used in these studies were highly swept; consequently, even small yaw angles caused the lee vortex to drift outboard, off the wing, reducing considerably the induced suction.

In this paper we present an experimental study of the effects of roll on the loading of a 60 deg swept delta wing. For this wing, which is typical of those used in both present and future aircraft configurations, the lee vortex is not swept off the wing even at high roll or yaw angles. The parameters studied are incidence angle, which included those in which VB was present for ϕ=0, and ground proximity. The experimental results will be compared with predictions obtained from an approximate model of the phenomenon.

The Experimental Installation

The experiments were carried out in the (1m x 1m) subsonic wind tunnel at the Technion Aeronautical Research Center. These experiments consisted of detailed surface pressure measurements as well as force and moment measurements.

The pressure measurements were carried out on the installation described in Ref. 3. The wing model is a 60° swept delta wing of 246 mm root chord, 4.6 mm thickness and beveled leading and trailing edges of 30° angle. The wing is equipped with 130 pressure ports on the starboard side of the upper surface in an arrangement shown in Fig. 1. The wing holder is attached to the lower surface, leaving the pressure measurement surface free of obstructions.

The pressure measurement system consists of three 48-port Scanivalve modules, each connected to a pressure transducer. The ground was simulated by a flat board 1.25 cm thick and 150 cm long, having a sharp leading edge and spanning the width of the wind tunnel parallel to the wind tunnel floor, starting approximately 100 cm upstream of the wing's leading-edge.

The pressure measurement procedure was dictated by the fact that the pressure ports are concentrated on one half of the upper surface. Consequently a complete surface pressure map for a given α and ϕ required four runs. To obtain the pressures on the upper planform measurements were taken at the given α and ϕ for the starboard (leading) side, and at α and $-\phi$ for the port (lee) side. To obtain pressures on the lower planform measurements were taken at α and $180+\phi$ for the starboard side, and at α and $180-\phi$ for the port side.

The force and moment measurements were carried out using a 6-component sting balance on a model having the same geometry as the one used for the pressure measurement, except for the wing holder. The holder for the force model is a faired central block protruding symmetrically from both the upper and lower surfaces, on which the balance is mounted. The force and moment measurements were carried out under the same conditions as the surface pressures.

Results and Discussion

The experiments were carried out at a free stream speed of 32 m/sec, and at 15 and 25 deg incidence. At each incidence, measurements were taken for ϕ=0, 15 and 25 degs, and $\bar{h}$=0.56 and 1.76.

Figure 2 illustrates the effects of roll on the surface pressures at the upper planform for α=15 deg. At this incidence, and for ϕ=0 deg, the wing is only marginally affected by VB ($\bar{x}_{VB} \cong 0.85$[4]). Roll affects both the position and magnitude of the vortex-induced suction peaks. The lee suction peak is displaced outward, while the leading suction peak is shifted inboard. The effects of roll on the suction peak magnitudes are influenced by VB. In the apex region (represented by $\bar{x}$=0.38), away from VB effects, the magnitude of the suction induced by the leading vortex increases while that induced by the lee vortex decreases. In the trailing-edge region (represented by $\bar{x}$=0.95), affected by VB, the effects of roll are reversed. In this region the roll-related effects of VB on the spanwise profile of the suction peaks appear to be weaker on the lee vortex and stronger on the leading one.

Figure 3 features the surface pressures at α=25 deg for ϕ=0 and 15 degs. For ϕ=0 deg, $\bar{x}_{VB} \cong 0.25$[4], and thus, the spanwise C_p profiles shown for this roll angle are affected by VB. In this case the magnitude of the lee suction peak increases and its spanwise profile appears to become less affected by VB. Thus, the weaker effects of VB on this vortex, as observed for this incidence angle and for the trailing-edge region at α=15 deg (Fig. 2) resulted in increased suction. On the other hand, the effects of VB on the spanwise profile of the leading vortex become more pronounced for larger roll angles and the magnitude of the suction peak decreases. Examination of the position of the suction peaks indicates that their spanwise displacement due to roll has a similar trend to that observed for α=15 deg.

Figure 4 features the effects of a further increase of ϕ, from 15 to 25 degs

at α=25 deg. The additional rolling angle resulted in a further displacement of the suction peaks in the same direction as that observed in the previous figure and a reduction in the magnitude of those peaks. The reduction in the magnitude of the leading suction peak, which appears to be affected by VB for these roll angles, is similar to that observed for this angle in Fig. 3. On the other hand, the reduction in the magnitude of the lee suction peak, which appears to be less affected by VB for these roll angles, is similar to that observed for this vortex at α=15 deg in the region unaffected by VB. This indicates that when the vortex is unaffected by VB, an increase in the roll angle results in a decrease in the suction peak induced by it.

Some of the above features are also evident in predictions obtained from an approximate model developed for delta wings in pitch and yaw (see Appendix A). Although this model neglects VB, it provides an indication and an explanation for some of the effects of roll on the aerodynamics of the wing. Table I presents the predicted effects of roll on the vortices' positions, circulations and the suction they induce on the wing for the conditions at which the measurements were taken (the coordinate transformation from that used for the approximate model to that used for the experimental data is given in Appendix A). The predictions show that due to roll, the leading vortex is displaced primarily downward and marginally inboard, its circulation remains approximately unchanged and the suction it induces on the wing increases. The lee vortex, on the other hand, is only marginally displaced (in both the spanwise and vertical directions), while the circulation as well as the induced suction decreases. Thus, the increased suction of the leading vortex can be attributed to its increased proximity to the wing surface, (since its circulation is unchanged) while the decreased suction of the lee vortex is a consequence of the decreased circulation (since its vertical position is virtually unchanged). Comparison of the predicted effects of roll on the suction peaks with the measured results (Figs. 2, 3 and 4) shows a qualitative agreement only when the vortices are free of VB effects. This is evident in Fig. 2, for the upstream region of the wing (represented by $\bar{x}$=0.38) and in Fig. 4 for the lee vortex. However, the predicted results may also indicate that the enhancement of VB effects due to increased roll observed experimentally on the leading vortex in Figs. 2, 3 and 4, are caused by the decrease in its height due to roll.

The rolling angle effects on the lower surface are marginal. This is highlighted in Fig. 5 which shows both that the magnitude of C_p on this surface are small and the variations due to roll are miniscule.

The effects of ground proximity on the pressures at the suction surface of the banked wing are presented in Fig. 6. The ground-free case is represented by $\bar{h}$=1.76 (at this height, ground proximity effects were shown[3] negligible for the wing used) and the ground-affected case is represented by $\bar{h}$=0.56. Results indicate that ground proximity increases the suction induced by the leading edge vortices, in a manner similar to that observed in Ref. (3) for a wing in pure pitch (ϕ=0 deg).

The Integral Characteristics

Both experimental and predicted results pertaining to the roll-induced effects on the wing loading appear in Table II. These results indicate that roll reduces the normal force acting on the wing. For α=15 deg, the measured reduction is similar to the predicted one, whereas at α=25 deg, where VB effects are significant, the measured reduction is larger than predicted.

The asymmetric, roll induced loading is evident in the difference in the normal force contributions, $\bar{C}_{NOR,1}$ and $\bar{C}_{NOR,2}$, of the two wing halves. In the present study, $\bar{C}_{NOR,1}$ is consistently larger than $\bar{C}_{NOR,2}$ for positive roll angles. This, in spite of the fact that roll enhanced VB effects on the leading half, and attenuated them on the lee half.

Examination of the rolling moment indicates that at α=15 deg, both the experimental and predicted coefficients are negative and decrease with increasing roll angle. On the other hand, at α=25 deg, the predicted coefficients are also negative and show the same trends as those at α=15 deg, while the measured values are positive. The difference between the measured C_R at α=25 deg from that measured at α=15 deg and from the predictions can be analyzed in view of the fact that the wing rolling moment is a balance between the positive sign contribution of the leading half-wing and the negative one of the lee half. The contribution of each half is the product of the normal force acting on it and the distance from its center of pressure to the rolling axis. Roll has two counteracting effects on the rolling moment of each wing half. On the leading half, roll increases the proportional share of the normal force, but reduces its distance to the rolling axis by

displacing the vortex induced suction peak inboard. On the lee side, roll effects are opposite. Since the roll-induced effects on $\bar{C}_{NOR,1}$ and $\bar{C}_{NOR,2}$ are similar at both α=15 and 25 degs, it can be deduced that the source of the wide variations in C_R is the roll-induced displacement of the centers of pressure of these two halves. At α=15 deg the negative C_R is consistent with a small displacement, whereas at α=25 deg, the positive C_R indicates increased displacement, sufficient to alter the direction of the rolling moment. The increased shift at α=25 deg is probably a consequence of VB which affects the leading edge vortices at this angle.

Summary

The present study illustrates the influence of VB on the rolling moment characteristics. For the 60 deg swept delta, from which the leading edge vortices are not swept off even at high roll angles, the presence of VB reduces the magnitude of $\left(\frac{\partial C_R}{\partial \phi}\right)$ considerably, and even alters its sign. This result should be taken into account when considering limits of maneuverability for aircraft with such wings.

Acknowledgement

The authors would like to thank Mr. Asaf Levin for his assistance in developing the approximate model.

References

1. Harvey, J.K., "Some Measurements on a Yawed Slender Delta Wing with Leading-Edge Separation", ARC R&M No. 3160, 1961.

2. Hummel, D., "Untersuchungen uber das Aufplatzen der Wirbel an Schlanken Deltaflugeln", Z. Flugwiss. Vol. 13, No. 5, 1965, pp. 155-168.

3. Er-El, J. and Weihs, D., "Ground Effect on Slender Wings Moderate and High Angles of Attack", ICAS Paper 84.2.8.2, Sept. 1984, and J. of Aircraft, Vol. 23, No. 5, 1986.

4. Wentz, W.J. Jr. and Kohlman, D.L., "Wind Tunnel Investigation of Vortex Breakdown on Slender Sharp-Edged Wings", Rep. FRL-68-013, University of Kansas Research Center, 1968.

5. Brown, C.E. and Michael, W.H., 1954, "Effect of Leading-Edge Separation on the Lift of a Delta Wing", J. Aeronaut. Sci., 21, pp. 690-694.

Appendix A

The approximate model used in the present study utilizes the approach proposed by Brown and Michael[5]. In this approach, it is assumed that the wing is slender and the flow about it is conical. The cross flow is governed by the two-dimensional Laplace equation in the y-z planes. The two leading edge vortices are represented as two concentrated vortices, each connected to the leading-edge by a feeding vortex sheet. The positions and the circulations of the vortices are determined from the requirements that the flow velocity at the leading-edge is finite (Kutta condition) and that the force acting on each vortex/feeding sheet system is zero.

In the present model, the flow in the cross plane is a flow with uniform sideslip about a plate and two vortices. The complex potential $W(\sigma)$ describing this flow is obtained by a Joukowsky transformation of the flow about a cylinder and two vortices (Fig. 7).

$$W(\sigma) = -\frac{i\Gamma_1}{2\pi}\ln\left[\frac{\frac{\sigma+\sqrt{\sigma^2-4a^2}}{2}-\zeta_1}{\frac{\sigma+\sqrt{\sigma^2-4a^2}}{2}-\frac{a^2}{\zeta_1}}\right] -$$

$$-\frac{i\Gamma_2}{2\pi}\ln\left[\frac{\frac{\sigma+\sqrt{\sigma^2-4a^2}}{2}-\zeta_2}{\frac{\sigma+\sqrt{\sigma^2-4a^2}}{2}-\frac{a^2}{\zeta_2}}\right]$$

$$-iV\alpha'\left[\frac{\sigma+\sqrt{\sigma^2-4a^2}}{2}-\frac{2a^2}{\sigma+\sqrt{\sigma^2-4a^2}}\right] -$$

$$-iV\beta'\left[\frac{\sigma+\sqrt{\sigma^2-4a^2}}{2}-\frac{2a^2}{\sigma+\sqrt{\sigma^2-4a^2}}\right] \qquad (1)$$

The Kutta condition gives the following relation:

$$\frac{i\Gamma_e}{2\pi}\left[\frac{1}{a-\zeta_1}-\frac{1}{a-\frac{a^2}{\zeta_1}}\right]+$$

$$+\frac{i\Gamma_a}{2\pi}\left[\frac{1}{a-\zeta_2}-\frac{1}{a-\frac{a^2}{\zeta_2}}\right]+i\cdot V\alpha'\cdot 2=0 \qquad (2a)$$

$$\frac{i\Gamma_e}{2\pi}\left[\frac{1}{a+\zeta_1}-\frac{1}{a+\frac{a^2}{\zeta_1}}\right]+$$

$$+\frac{i\Gamma_a}{2\pi}\left[\frac{1}{a+\zeta_2}-\frac{1}{a+\frac{a^2}{\zeta_2}}\right]-i\cdot V\alpha'\cdot 2=0 \qquad (2b)$$

while from the zero force condition, we get

$$i\cdot\rho\cdot\Gamma_1\left[-V_1^*+V\cdot\epsilon\cdot\left(\frac{2\sigma_1-2a}{2a}\right)\right]=0 \qquad (3a)$$

$$i\cdot\rho\cdot\Gamma_2\left[-V_2^*+V\cdot\epsilon\cdot\left(\frac{2\sigma_2-2a}{2a}\right)\right]=0 \qquad (3b)$$

where

$$V_1^*=\left(\frac{\bar{\sigma}_1}{a}-1\right)\cdot V\cdot\varepsilon \qquad (4a)$$

and

$$V_2^*=\left(\frac{\bar{\sigma}_2}{a}+1\right)\cdot V\cdot\varepsilon \qquad (4b)$$

Equations (2), (3) and (4) determine the position and circulation of both leading edge vortices.

The pressure distribution is determined from

$$p=p_\infty-\frac{1}{2}\rho V^2\left[\frac{2\varphi_x}{V}+\frac{\varphi_y^2}{V^2}+\frac{\varphi_z^2}{V^2}-\alpha^2\right], \qquad (5)$$

the normal force is obtained from

$$L=-\rho V\,\mathrm{Real}\left[\oint W(\zeta)\frac{d\sigma}{d\zeta}d\zeta\right], \qquad (6)$$

and the rolling moment is given by

$$M_R=\frac{\rho}{2}\left\{V\cdot\mathrm{Real}\left[\oint W(\sigma)d(\sigma\bar{\sigma})\right]+\right.$$

$$\left.+\mathrm{Real}\left[\int_0^c dx\oint\left(\frac{dw}{d\sigma}\right)\right]\right\} \qquad (7)$$

Although this model was developed for a wing in pitch and yaw (with no roll), it can also be utilized for a wing in equivalent pitch and roll (with no yaw), after transformation of the coordinate system using the following relations

$$V_\infty'=V_\infty\cdot\cos\alpha$$

$$\alpha'=\tan\alpha\cdot\cos\phi \qquad (8)$$

$$\beta'=-\tan\alpha\cdot\sin\phi$$

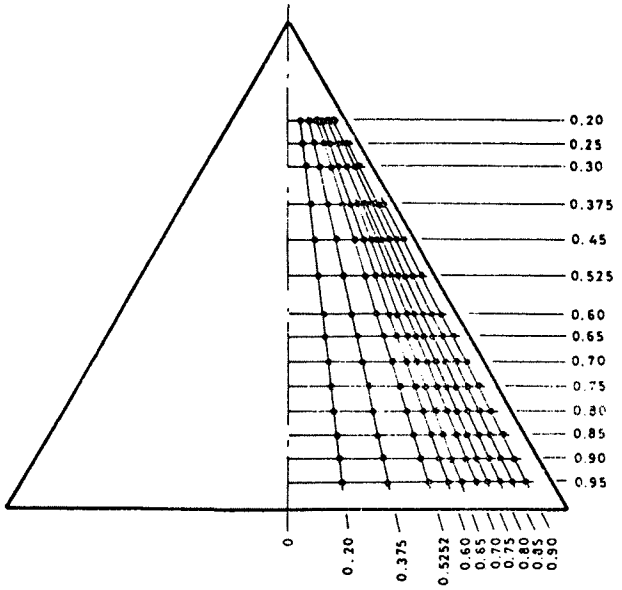

Fig. 1. Map of pressure measurement ports.

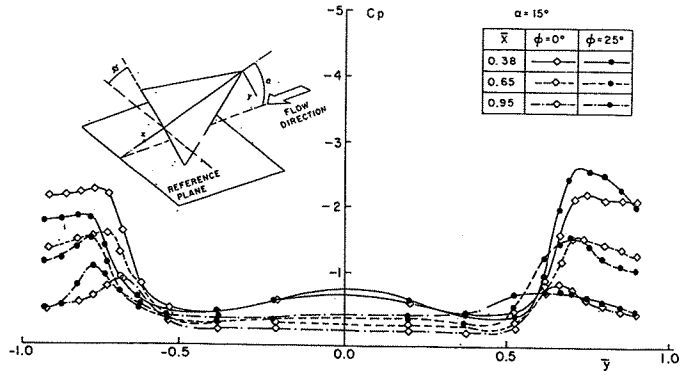

Fig. 2. Effect of roll on the pressures at the upper surface.

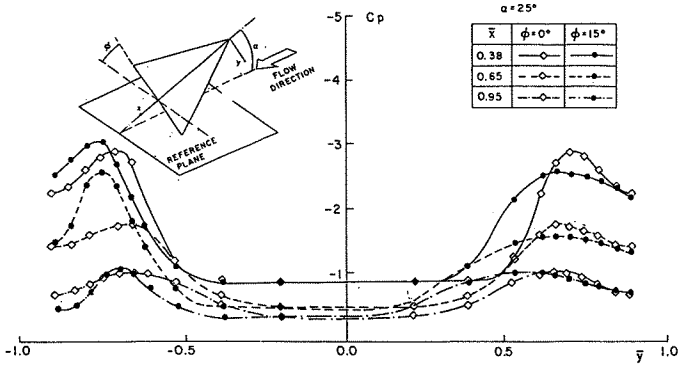

Fig. 3. Effect of roll on the pressures at the upper surface.

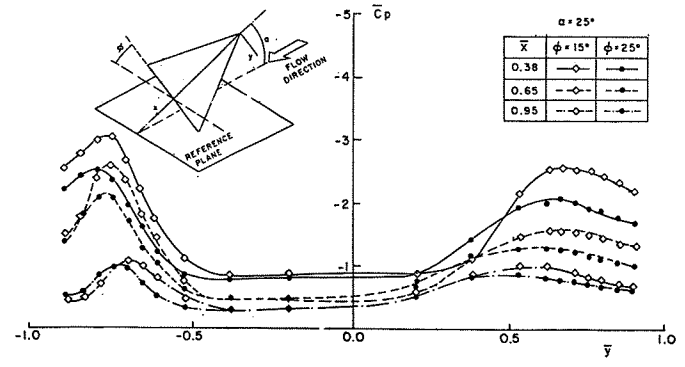

Fig. 4. Effect of roll on the pressures at the upper surface.

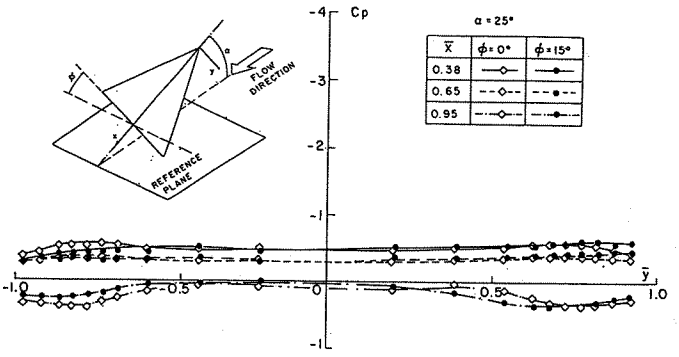

Fig. 5. Effect of roll on the pressure at the lower surface.

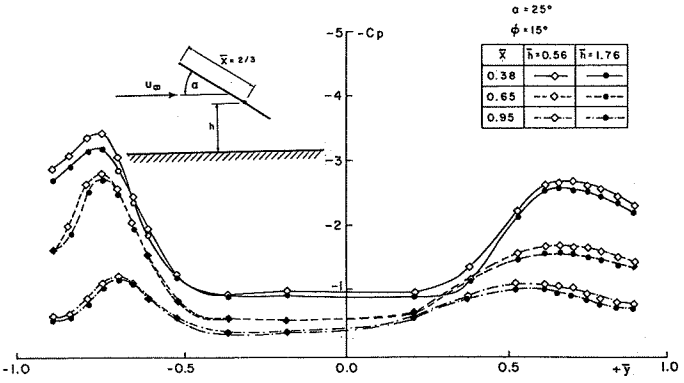

Fig. 6. Effect of ground proximity on the pressure at the upper surface; α=25deg, ϕ=15 deg..

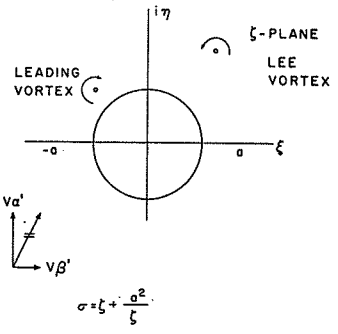

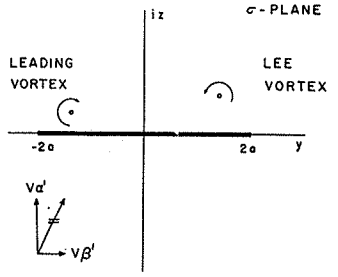

Fig. 7. The cross flow plane.

Table I

Predicted effects of roll on the leading edge vortices

		Lee Vortex				Leading Vortex			
α	ϕ	$\frac{\bar{y}(\phi)}{\bar{y}(\phi=0)}$	$\frac{\bar{z}(\phi)}{\bar{z}(\phi=0)}$	$\frac{\Gamma(\phi)}{\Gamma(\phi=0)}$	$\frac{C_{p,min}(\phi)}{C_{p,min}(\phi=0)}$	$\frac{\bar{y}(\phi)}{\bar{y}(\phi=0)}$	$\frac{\bar{z}(\phi)}{\bar{z}(\phi=0)}$	$\frac{\Gamma(\phi)}{\Gamma(\phi=0)}$	$\frac{C_{p,min}(\phi)}{C_{p,min}(\phi=0)}$
15	15	1.006	1.008	.916	0.845	.998	.927	.999	1.143
	25	1.012	.975	.827	.749	.999	.848	.952	1.231
25	15	1.018	1.032	.896	.779	.989	.910	1.017	1.225
	25	1.033	1.018	.790	.637	.987	.824	.976	1.367

Table II

Effects of roll and ground proximity on C_{NOR} and C_R

		$\frac{C_{NOR(\phi)}}{C_{NOR(\phi=0)}}$		C_R				Ground Effect	
α	ϕ	measured	predicted	measured	predicted	$\bar{C}_{NOR,2}$	$\bar{C}_{NOR,1}$	$\frac{C_{NOR}(\bar{h}=.56)}{C_{NOR}(\bar{h}=1.76)}$	$\frac{C_R(\bar{h}=.56)}{C_R(\bar{h}=1.76)}$
15	15	.96	.97	- .044	- .031	.47	.53	1.06	1.07
	25	.89	.89	- .091	- .047	.45	.55	1.06	1.28
25	15	.94	.96	.010	- .091	.47	.53	1.07	2.46
	25	.83	.91	.002	- .137	.45	.55	1.12	3.11